

Microfluidics Synthesis of Gene Silencing Cubosomes

Hojun Kim^{§,†}, Jaek Sung[§], Yunju Chang[§], Alana Alfeche[§], Cecilia Leal^{§,*}

[§]Materials Science and Engineering Department, University of Illinois at Urbana-Champaign,
1304 West Green Street, Urbana, Illinois 61 801, United States.

[†]Center for Biomaterials, Biomedical Research Institute, Korea Institute of Science and
Technology (KIST), Seoul, Republic of Korea

*Correspondence and requests for materials should be addressed to Cecilia Leal (email:

cecilial@illinois.edu)

Note 1. Ethanol-in-Water Droplet Properties: Figure S1 shows the effect of lipid concentration and flow properties on the ethanol-in-water droplets. The droplets are stabilized by a lipid bilayer as schematically represented in Fig. S1A. Figure S1A represents Dynamic Light Scattering (DLS) elucidating droplet size as a function of lipid concentration. The polydispersity index (PDI) is also presented in a second Y axis (blue). For lipid concentrations of 1mM, 10 mM, and 100mM, average emulsion diameters of 46, 48, and 77 nm are obtained, respectively. As previously observed for different lipid systems, larger emulsion sizes relate to higher lipid concentration.¹ The PDI is barely affected by lipid concentration being 0.05, 0.05, and 0.06 for 1, 10, and 100 mM lipid concentration, respectively. Figure S1B shows that for higher flow rate and flow rate ratio (water /lipid solution) smaller droplets are obtained (at 10 mM lipid concentration). For these microfluidic devices a stable behavior was found at a fixed flow rate ratio of 4 and flow rate of 0.05 ml/min.

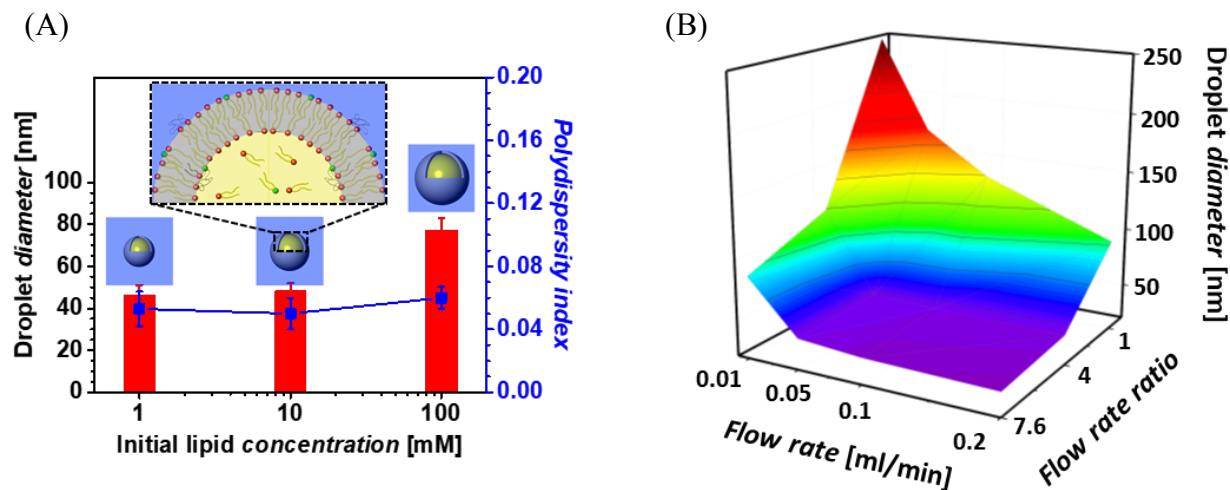


Figure S1. Droplets eluted from the SHM device were collected and characterized by DLS at various flow conditions and lipid concentrations. (A) DLS measurements of emulsion solutions from different initial lipid concentrations (1, 10, and 50 mM) fabricated at flow rate ratio and flow rate of 0.05 ml/min and 4. Increasing lipid concentration leads to increase of emulsion sizes (46, 48, and 77 nm), while the polydispersity index is not significantly affected (0.05, 0.05, and 0.06). (B) Average droplet diameter as a function of flow conditions. The size characteristics are saturated (~48 nm) at flow rate and flow rate ratio of 0.05 ml/min and 4, respectively.

Note 2. Dynamic Light Scattering of Microfluidic Cubosomes and Cuboplexes: Figure S2 shows the DLS data indicating that cubosome size and polydispersity is not significantly affected by siRNA incorporation.

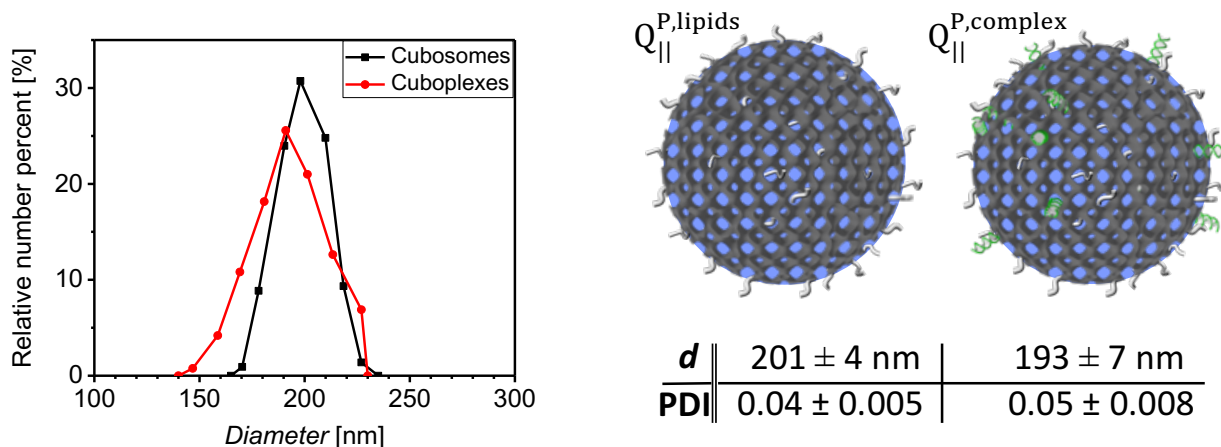


Figure S2. Size characteristics of cubosomes and cuboplexes. Cubosomes are made by microfluidics device at total flow rate and flow rate ratio of 0.05 ml/min and 4 (water / lipid solution). siRNA was encapsulated into the cubosomes (GMO/DOTAP/GMOPEG of 97/2/1, mole ratio) post cubosome synthesis. (A) DLS data of cubosomes and cuboplexes show monomodal distributions. siRNA inclusion induces only a slight peak broadening and shift to to smaller average size. (B) schematics of cubosome and cuboplex and DLS data summary. Inclusion of siRNAs in cubosomes decreases the average particle size from 201 nm to 193 nm with slight increase of polydispersity index (from 0.04 to 0.05).

Note 3. Mapping of siRNA partition in cubosomes membranes: Figure S3A shows a magnified Cryo-EM image where the lipid membranes are marked by white dash-lines and the locations of darker siRNA-AuNP are marked by yellow dots. In Figure S3B the linear electron density along specific lines in the image are presented.

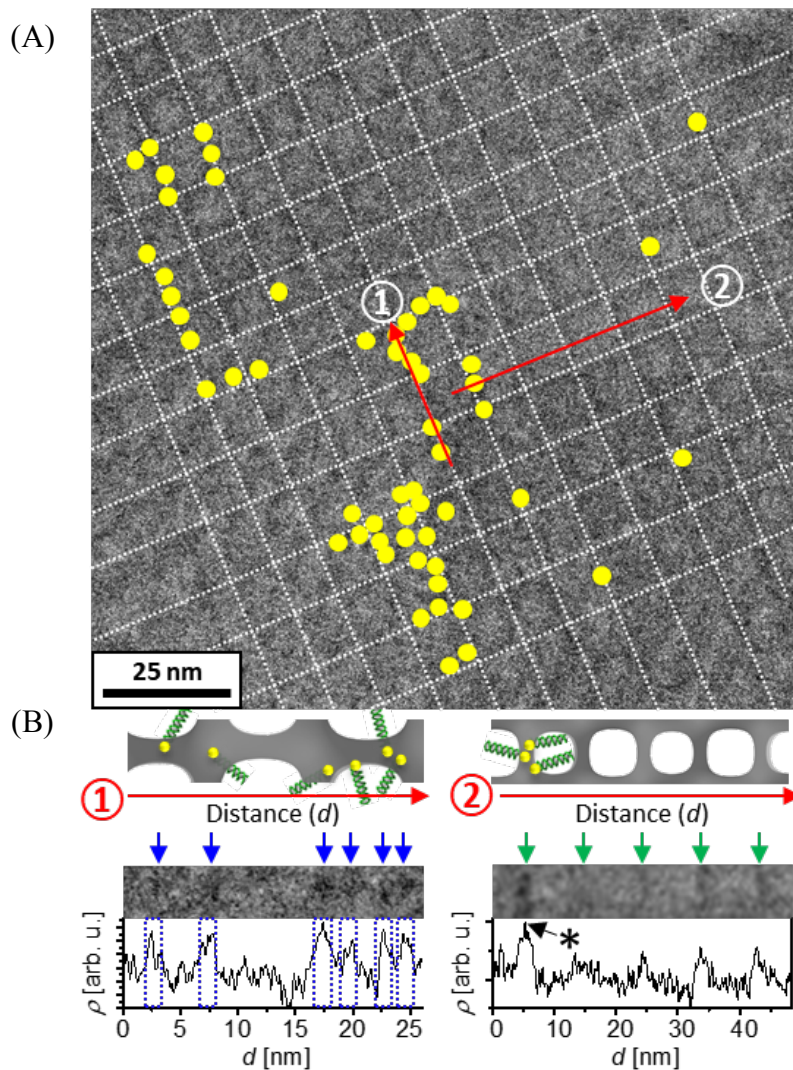


Figure S3. siRNA locations in the lipid cubic phase matrix of cubosomes are mapped out using 1D electron density profiles. (A) Cryo-EM image of a zoomed-in cuboplex (GMO/DOTAP/GMOPEG of 97/2/1, mole ratio) having 1.8 nm diameter gold nanoparticle-siRNA conjugates (siRNA-AuNP) at neutral charge ratio ($\rho = 1$). The locations of gold nanoparticles and lipid membranes are marked as yellow dots and white grid lines, respectively. It was found that gold nanoparticles are aligned through the water channels and at close proximity to lipid membranes presumably due to the electrostatic attraction between siRNAs and DOTAP. (B) 1D electron density profile analysis to identify the locations of siRNA-AuNP conjugates. Two lines (red arrow in Figure S2A) are chosen and 1D electron density profiles are obtained from the image using the Gatan Microscopy Suite software. On the left graph, there are six high electron density locations (blue arrows) that are mapped to the location of siRNA-AuNP conjugates. On

the right image, three gold nanoparticle-siRNA conjugates are found at the proximity of the left membrane, giving considerably higher electron density contrast than the next four lipid membranes (green arrows) without gold siRNA-AuNP.

Note 4. Two-dimensional electron density profile images: Figure S4 shows additional 2D electron density maps of cubosomes and cuboplexes.

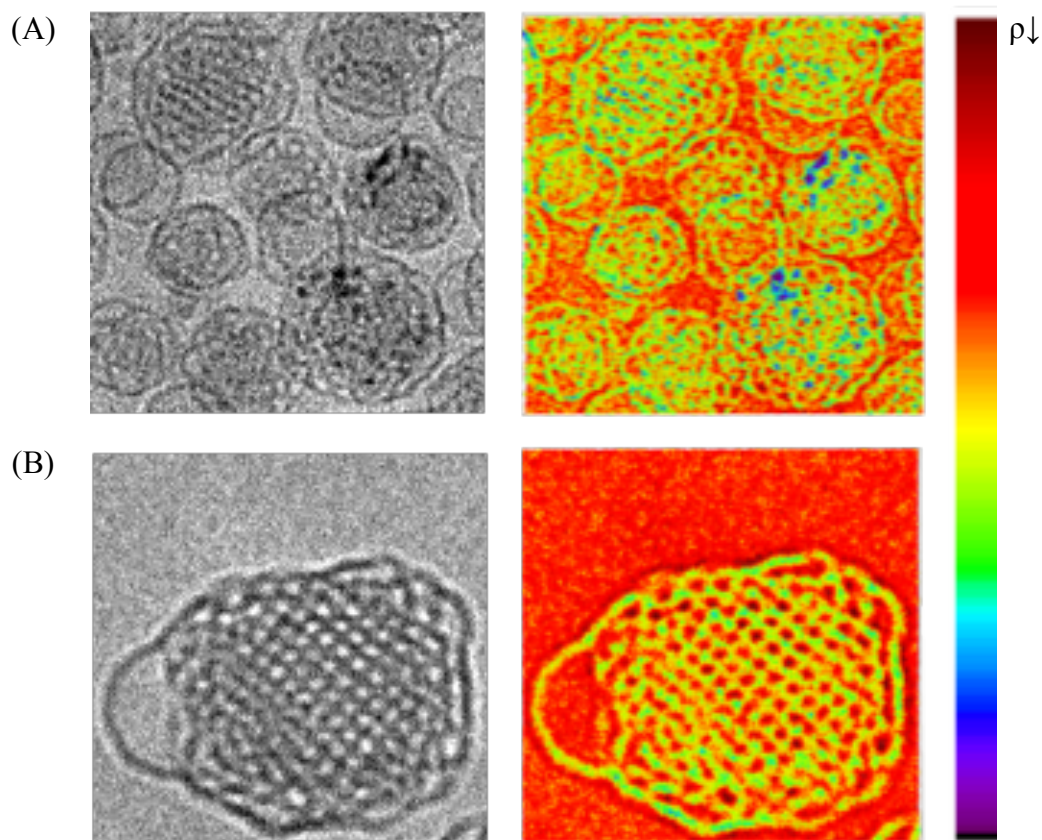


Figure S4. Two-dimensional Cryo-EM images and corresponding electron density profile of small cuboplexes and cubosomes (GMO/DOTAP/GMOPEG of 96/2/2, mole ratio). (A) Cuboplexes with gold siRNA-AuNP. On the right image, blue regions (high electron contrast) indicates the location of AuNPs. (B) Cubosome and its electron density map. Compared to (A), only red and green colors are found, indicating that there are only water and lipid membranes in the system. *Image size: (A) 140 nm x 140 nm, (B) 190 nm x 190 nm

References

1. Carugo, D., Bottaro, E., Owen, J., Stride, E. & Nastruzzi, C. Liposome Production by Microfluidics: Potential and Limiting Factors. *Sci. Rep.* **2016**, *6*, 25876-25891.